C-X-C receptor 7 agonist acts as a C-X-C motif chemokine ligand 12 inhibitor to ameliorate osteoclastogenesis and bone resorption

ALEXANDER PATERA NUGRAHA[1,2*], HIDEKI KITAURA[1], FUMITOSHI OHORI[1*], ADYA PRAMUSITA[1], SAIKA OGAWA[1], TAKAHIRO NOGUCHI[1], ASEEL MARAHLEH[1], YASUHIKO NARA[1], RIA KINJO[1] and ITARU MIZOGUCHI[1]

[1]Division of Orthodontics and Dentofacial Orthopedics, Tohoku University Graduate School of Dentistry, Aoba-ku, Sendai, Miyagi 980-8575, Japan; [2]Orthodontics Department, Faculty of Dental Medicine, Airlangga University, Surabaya 60132, Indonesia

Received September 6, 2021; Accepted December 9, 2021

DOI: 10.3892/mmr.2022.12594

Abstract. The C-X-C receptor (CXCR) 7 agonist, VUF11207, is a chemical compound that binds specifically to CXCR7, and negatively regulates C-X-C motif chemokine ligand 12 (CXCL12) and CXCR4-induced cellular events. Lipopolysaccharide (LPS) can induce inflammatory cytokines and pathological bone loss. LPS also induces expression of CXCL12, enhancing sensitivity to receptor activator of NF-κB ligand (RANKL) and tumor necrosis factor-α (TNF-α) *in vivo*. RANKL and TNF-α induce the differentiation of osteoclasts into osteoclast precursors and bone resorption. The current study was performed to examine the effects of a CXCR7 agonist on osteoclastogenesis and bone resorption induced by LPS *in vivo*. In addition, the mechanisms underlying these *in vivo* effects were investigated by *in vitro* experiments. Eight-week-old male C57BL/6J mice were subcutaneously injected over the calvariae with LPS alone or LPS and CXCR7 agonist. After sacrifice, the number of osteoclasts and the bone resorption area were measured. *In vitro* experiments were performed to investigate the effects of CXCL12 and CXCR7 agonist on osteoclastogenesis induced by RANKL and TNF-α. Mice injected with LPS and CXCR7 agonist showed significantly reduced osteoclastogenesis and bone resorption compared with mice injected with LPS alone. Moreover, the CXCR7 agonist inhibited CXCL12 enhancement of RANKL- and TNF-α-induced osteoclastogenesis *in vitro*. Thus, CXCR7 agonist inhibited LPS-induced osteoclast-associated cytokines, such as RANKL and TNF-α, as well as RANKL- and TNF-α-induced osteoclastogenesis *in vitro* by modulating CXCL12-mediated enhancement of osteoclastogenesis. In conclusion, CXCR7 agonist reduced CXCL12-mediated osteoclastogenesis and bone resorption.

Correspondence to: Dr Hideki Kitaura, Division of Orthodontics and Dentofacial Orthopedics, Tohoku University Graduate School of Dentistry, 4-1 Seiryo-Machi, Aoba-ku, Sendai, Miyagi 980-8575, Japan
E-mail: hideki.kitaura.b4@tohoku.ac.jp

*Contributed equally

Key words: C-X-C receptor 7 agonist, C-X-C motif chemokine ligand 12, receptor activator of NF-κB ligand, tumor necrosis factor-α, osteoclast

Introduction

Osteoclasts are multinucleated cells formed by the fusion of hematopoietic bone marrow precursors and are typically present in the bone marrow adjacent to the bone surface (1). Osteoclasts play a pivotal role in bone resorption in several bone-related diseases, such as rheumatoid arthritis and periodontitis (2,3). Receptor activator of NF-κB ligand (RANKL), macrophage colony stimulating factor (M-CSF) and tumor necrosis factor (TNF)-α are cytokines known to promote osteoclastogenesis *in vitro* and *in vivo* (4-6).

Lipopolysaccharide (LPS) can induce inflammatory cytokine production and pathological bone loss (7). Various inflammatory cytokines induced by LPS, such as TNF-α, play important roles in the maturation of osteoclast progenitors (8,9). These cytokines are related to osteoclastogenesis and bone resorption induced by LPS *in vitro* and *in vivo* (10). Furthermore, LPS may also lead to osteoclastogenesis and promote the fusion and survival of osteoclasts (11). In addition, the expression of RANKL in osteoblasts is stimulated by LPS (12).

Chemokines, which are various small chemotactic cytokines, are potentially related to the physiological development, pathological recruitment and function of osteoclasts (13-15). C-X-C motif chemokine ligand 12 (CXCL12) is widely recognized as stromal cell-derived factor 1 and belongs to the CXC chemokine family. CXCL12 is a 68-residue chemokine with a molecular weight of 8 kDa that exists in both secreted and membrane-bound forms, and is abundantly expressed in bone marrow and several other tissues (16,17). CXCL12 has strong chemotactic effects on lymphocytes and has been shown to be associated with osteoclast progenitor cell survival, function and fusion (18,19).

The crucial roles of CXCR4 and its ligand CXCL12 have been extensively studied (20). CXCR4 is a 352-residue G protein-coupled receptor with seven transmembrane helices (21). CXCR4 is broadly expressed by both mononuclear cells and progenitor cells in the bone marrow (18). CXCL12 was shown to indirectly increase osteoclastogenesis and bone resorption *in vivo* by LPS-stimulated TNF-α in macrophages, and LPS-enhanced RANKL in osteoblasts in mice injected with LPS (22). Furthermore, CXCL12 was shown to directly enhance both RANKL- and TNF-α-induced osteoclastogenesis (22). As shown in studies using the CXCR4 antagonist, AMD3100, the interaction of CXCL12 and CXCR4 induces osteoclastogenesis and regulates osteoclast function (18,23,24).

CXCR7 is a G protein-coupled receptor with seven membrane-spanning helices (16). A previous study showed that a CXCR7 agonist negatively regulates CXCL12-CXCR4-induced cellular events, such as angiogenesis (25). However, the functions and roles of CXCR7 in this process remain unclear. To understand the mechanisms of bone resorption relevant to disease, it is important to investigate the role of CXCR7 agonists in LPS-induced osteoclastogenesis. However, to the best of our knowledge, there have been no studies to evaluate the effects of CXCR7 agonists on osteoclastogenesis induced by LPS *in vivo*. Therefore, the present study was performed to investigate the effects of the CXCR7 agonist, VUF11207, on LPS-induced osteoclastogenesis in an animal model *in vivo*.

Materials and methods

Reagents and animals. A total of 20 8-10-week-old healthy 20-25 g male C57BL/6J mice (wild-type/WT) purchased from CLEA Japan, Inc., were used. Mice were kept in cages that were maintained at 25˚C, 50% relative humidity under a 12 h light/dark cycle with free access to food and water. A total of five mice were assigned to each experimental group by simple random sampling. All experimental procedures conformed to 'Regulations for Animal Experiments and Related Activities at Tohoku University', and were reviewed by the Institutional Laboratory Animal Care and Use Committee of Tohoku University and approved by the President of Tohoku University (approval no. 2019DnA-047-05; Miyagi, Japan).

CXCL12 was obtained from R&D Systems, Inc. The CXCR7 agonist, VUF11207, was purchased from MilliporeSigma. LPS from *Escherichia coli* was purchased from Sigma-Aldrich (Merck KGaA). Recombinant mouse RANKL (26) and TNF-α (27) were produced as described previously. Recombinant mouse M-CSF was produced by the M-CSF-expressing cell line, CMG14-12, as described previously (28).

Mouse experiments and histological examination. Mice in each group received subcutaneous injections over the crown of the head for 5 days with one of the following: i) Phosphate-buffered saline (PBS, 100 μl); ii) LPS (100 μg/day); iii) LPS (100 μg/day) + CXCR7 agonist (100 μg/day); or iv) CXCR7 agonist (100 μg/day).

The mice were sacrificed by inhalation of an overdose of 5% isoflurane on day 6. Inhalation was continued until a pulse could not be detected, breathing had ceased and there was an absence of reflexes observed in combination. The calvariae of mice were isolated and cut into three pieces. After fixation with 4% formaldehyde in PBS at 4˚C for 3 days, the samples were demineralized in 14% EDTA for 3 days. The samples were embedded in paraffin blocks and cut into sections 5-μm thick using a microtome (REM-710; Yamato Kohki Industrial Co., Ltd.). The sections were stained for tartrate-resistant acid phosphatase (TRAP) and counterstained with hematoxylin according to the protocol described previously (22,29). Osteoclasts were recognized as TRAP-positive cells with more than three nuclei. The number of TRAP-positive cells (cells/section) was counted in the sagittal sutures of calvariae according to previously described methods (22,29,30).

Measurement of bone destruction. Mice were injected as described above and sacrificed on day 6. Bone destruction was assessed by micro-computed tomography (CT) (ScanXmate-E090; Comscantecno Co., Ltd.). The dissected calvariae were fixed with 4% formaldehyde in PBS at 4˚C for 3 days. The calvariae were scanned by micro-CT to create three-dimensional images using TRI/3D-BON64 version R7.00 software (Ratoc System Engineering Co., Ltd.). The bone resorption areas were measured around the bregma 45 pixels in the sagittal plane and 50 pixels in the coronal plane. The bone resorption areas (%) to total areas were measured using ImageJ version 1.51 (National Institutes of Health) as described previously (22,29,30). Shaded areas of the same color density were considered bone resorption areas.

Preparation of RNA and reverse transcription-quantitative polymerase chain reaction (RT-qPCR) analysis. Mice received subcutaneous injections into the crown of the head for 5 days as described above. The mice were then sacrificed, and their calvariae were isolated, frozen in liquid nitrogen and homogenized (Micro Smash MS-100R; Tomy Seiko Co., Ltd.). Total RNA was obtained from samples using TRIzol reagent (Invitrogen; Thermo Fisher Scientific, Inc.). Total RNA was purified by the RNeasy Mini Kit (Qiagen, Inc.). After purification of total RNA, cDNA was synthesized from each total RNA sample (2 μg) with oligo(dT) primers by using the SuperScript IV First-Strand Synthesis System according to the manufacturer's protocol (Invitrogen; Thermo Fisher Scientific, Inc.). The levels of TRAP, Cathepsin K, RANKL and TNF-α transcripts were quantified by qPCR (Thermal Cycler Dice Real Time system; Takara Bio, Inc.). The reaction consisted of a volume of 25 μl containing 2 μl cDNA as a template, 23 μl TB Green Premix Ex Taq II (Takara Bio, Inc.) and 50 pmol/μl each primer. The thermocycling conditions consisted of an initial denaturation step at 95˚C for 10 sec, followed by 50 cycles of denaturation for 5 sec at 95˚C and annealing for 30 sec at 60˚C. The levels of glyceraldehyde 3-phosphate dehydrogenase (GAPDH) mRNA were used for normalization. Relative expression of mRNA was analyzed by the $2^{-\Delta\Delta Cq}$ method (31). All primers were designed by our laboratory (Division of Orthodontics and Dentofacial Orthopedics, Tohoku University Graduate School of Dentistry). The primers used for analysis are listed in Table I. Preparation of osteoclast precursors and cultures for osteoclastogenesis. Mouse bone marrow cells were used for the *in vitro* study. After sacrifice, the femora and tibiae of mice were dissected aseptically. Both ends of these bones were

Table I. Primers used in this study.

Gene	Sequence (5'→3')	Genbank number	Size, bp	Tm, ˚C
GAPDH	F: GGTGGAGCCAAAAGGGTCA	XM_017321385.1	138	67.3
	R: GGGGGCTAAGCAGTTGGT			64.0
TRAP	F: AACTTGCGACCATTGTTA	XM_011242384.2	159	56.5
	R: GGGGACCTTTCGTTGATGT			63.7
Cathepsin K	F: GCAGAGGTGTGTACTATGA	BC046320.1	73	50.3
	R: GCAGGCGTTGTTCTTATT			57.8
RANKL	F: CCTGAGGCCCAGCCATTT	NM_011613.3	107	63.9
	R: CTTGGCCCAGCCTCGAT			66.5
TNF-α	F: CTGTAGCCCACGTCGTAGC	NM_013693.3	97	56.4
	R: TTGAGATCCATGCCGTTG			53.9

F, forward; R, reverse; Tm, temperature; TRAP, tartrate-resistant acid phosphatase; RANKL, receptor activator of NF-κB ligand; TNF-α, tumor necrosis factor-α.

cut off to obtain bone marrow cells. Bone marrow cells were seeded ($5x10^6$ cells) into 10-cm culture dishes with α-modified minimal essential medium (α-MEM; FUJIFILM Wako Pure Chemical Corporation) containing 100 ng/ml M-CSF, 10% fetal bovine serum (FBS; Biowest, Inc.), 100 IU/ml penicillin G (Meiji Seika Kaisha, Ltd.) and 100 μg/ml streptomycin (Meiji Seika Kaisha, Ltd.). Bone marrow cells were incubated at 37˚C in 5% CO_2 for 4 days. Floating cells were eliminated by rinsing with PBS. After elimination of floating cells, adherent cells were detached using trypsin/EDTA solution (Sigma-Aldrich; Merck KGaA) and collected. The obtained cells were recognized as osteoclast precursors (22,29,30). Osteoclast precursors were seeded into 96-well plates and cultured in an atmosphere of 5% CO_2 at 37˚C for 5 days containing the following for RANKL analysis: i) M-CSF (100 ng/ml); ii) M-CSF (100 ng/ml) + RANKL (50 ng/ml); iii) M-CSF (100 ng/ml) + RANKL (50 ng/ml) + CXCL12 (100 ng/ml); iv) M-CSF (100 ng/ml) + RANKL (50 ng/ml) + CXCL12 (100 ng/ml) + CXCR7 agonist (100 ng/ml); v) M-CSF (100 ng/ml) + RANKL (50 ng/ml) + CXCR7 agonist (100 ng/ml); or vi) M-CSF (100 ng/ml) + CXCR7 agonist (100 ng/ml). Cultures for TNF-α analysis contained the following: i) M-CSF (100 ng/ml); ii) M-CSF (100 ng/ml) + TNF-α (50 ng/ml); iii) M-CSF (100 ng/ml) + TNF-α (50 ng/ml) + CXCL12 (100 ng/ml); iv) M-CSF (100 ng/ml) + TNF-α (50 ng/ml) + CXCL12 (100 ng/ml) + CXCR7 agonist (100 ng/ml); v) M-CSF (100 ng/ml) + TNF-α (50 ng/ml) + CXCR7 agonist (100 ng/ml); or vi) M-CSF (100 ng/ml) + CXCR7 agonist (100 ng/ml). After fixation with 4% formaldehyde at room temperature for 1 h, the cultured cells were stained with TRAP as described previously (22,29,30). Osteoclasts were identified as TRAP-positive cells with three or more nuclei. The number of osteoclasts (cells/well) was counted under a light microscope.

Immunoblotting. Osteoclast precursors prepared from bone marrow cells were incubated for 6 h ($5x10^6$ cells) in 60-mm cell culture dishes (Corning, Inc.) using serum-free α-MEM for culture under conditions of serum starvation. After serum starvation for 6 h, osteoclast precursors were cultured with the following for RANKL analysis: i) RANKL (100 ng/ml); ii) RANKL (100 ng/ml) + CXCL12 (100 ng/ml); or iii) RANKL (100 ng/ml) + CXCL12 (100 ng/ml) + CXCR7 agonist (100 ng/ml). Cultures for TNF-α analysis contained the following: i) TNF-α (100 ng/ml); ii) TNF-α (100 ng/ml) + CXCL12 (100 ng/ml); or iii) TNF-α (100 ng/ml) + CXCL12 (100 ng/ml) + CXCR7 agonist (100 ng/ml). They were added to the dishes for specific periods (0, 15 or 30 min). Osteoclast precursors treated with the specified reagents were gently rinsed twice with PBS. Radioimmunoprecipitation (RIPA) lysis buffer (MilliporeSigma) with phosphatase inhibitor and 1% protease (Thermo Fisher Scientific, Inc.) was added to the cell culture dishes. The cells were scraped from the dishes. Measurement of total protein concentrations was performed using a Pierce BCA protein assay kit (Thermo Fisher Scientific, Inc.). β-Mercaptoethanol and Laemmli sample buffer (Bio-Rad Laboratories, Inc.) were added to protein samples. The samples were denatured at 95˚C for 5 min for SDS-PAGE. The same amounts of proteins (40 μg) and marker were loaded into the wells using 4-15% Mini-PROTEAN TGX Precast Gels (Bio-Rad Laboratories, Inc.) and the gels were run at 120 V for 1 h. The proteins were transferred from the gels onto polyvinylidene difluoride (PVDF) membranes using a PVDF Trans-Blot Turbo Transfer System (Bio-Rad Laboratories, Inc.). After transfer, nonspecific binding sites on the membranes were blocked by incubation with Block-Ace (KAC Co., Ltd.) at room temperature for 120 min. After blocking, the membranes were reacted overnight at 4˚C with the following primary antibodies (all, 1:1,000): Monoclonal anti-β-actin mouse antibody (cat. no. A1978; Sigma-Aldrich; Merck KGaA), phosphorylated (p)-p44/42 MAPK (Erk1/2) antibody (cat. no. 9101), p44/42 (Erk1/2) antibody (cat. no. 9102), p-p38 MAPK rabbit monoclonal antibody (cat. no. 4511), p38 MAPK antibody cat. no. 9212, p-SAPK/JNK rabbit monoclonal antibody (cat. no. 4671) and SAPK/JNK antibody (cat. no. 9252; Cell Signaling Technology, Inc.). The membranes were washed with Tris buffered saline (TBS) and TBS with Triton X-100 (TBST) with gentle agitation. The membranes were incubated at room temperature for 60 min with HRP-conjugated anti-rabbit IgG antibody (cat. no. 7074; Cell Signaling Technology, Inc.; 1:3,000) and anti-mouse antibody (cat. no. NA931; GE Healthcare; 1:10,000) as secondary

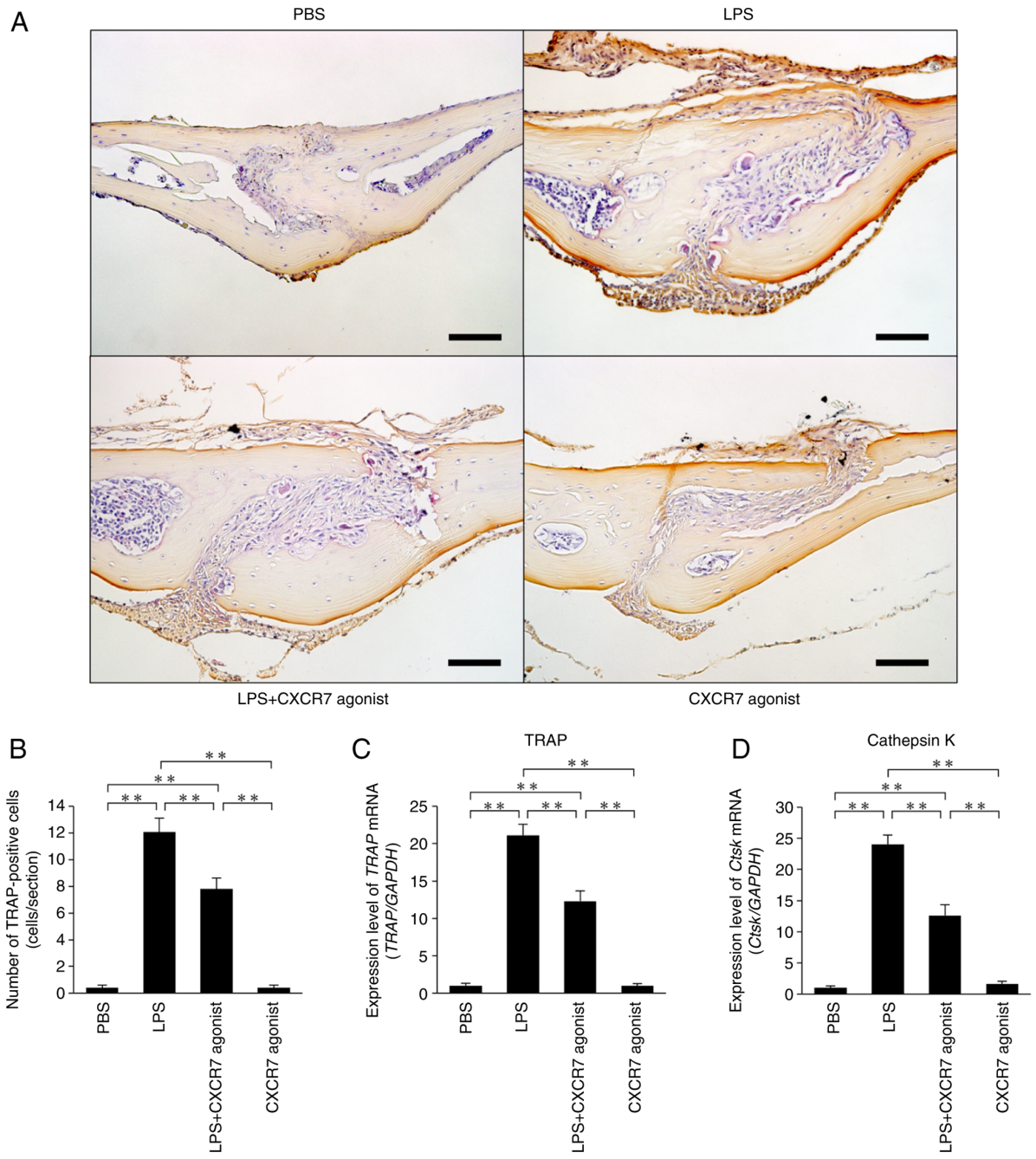

Figure 1. CXCR7 agonist acts as a C-X-C motif chemokine ligand 12 inhibitor and ameliorates LPS-induced bone resorption. (A) Histological sections of mouse calvariae stained for TRAP and counterstained with hematoxylin. TRAP-positive cells were stained red. Scale bar, 50 μm. (B) Number of osteoclasts in the suture of mouse calvariae. (C) TRAP and (D) Cathepsin K mRNA transcript levels in mouse calvariae measured by reverse transcription-quantitative PCR. The statistical significance of differences was determined by one-way ANOVA followed by Bonferroni/Dunn's test (n=4; **P<0.01). Results are expressed as the mean ± SEM. CXCR7, C-X-C receptor 7; LPS, lipopolysaccharide; TRAP, tartrate-resistant acid phosphatase; PBS, phosphate-buffered saline.

antibodies. The membranes were washed in TBST and TBS with gentle agitation. After washing, SuperSignal West Femto Maximum Sensitivity Substrate (Thermo Fisher Scientific, Inc.) was added and incubated for 5 min. The signals on blots were imaged using the FUSION-FX7.EDGE Chemiluminescence Imaging System (Vilber Lourmat) (32).

Statistical analysis. All data are expressed as the mean ± standard error of the mean (SEM) of more than three independent experiments. All data were analyzed using Statcel version 3 software (OMS Publishing Co., Ltd.). Differences between groups were examined using one-way ANOVA followed by Bonferroni/Dunn's test. F-values are shown in Table SI. P<0.05 was considered to indicate a statistically significant difference.

Results

CXCR7 agonist inhibits LPS-induced osteoclastogenesis in vivo. LPS was administered for 5 consecutive days and calvariae were stained with TRAP to reveal osteoclast formation (Fig. 1A). Large numbers of osteoclasts formed in the sutures of calvariae in LPS-injected mice compared

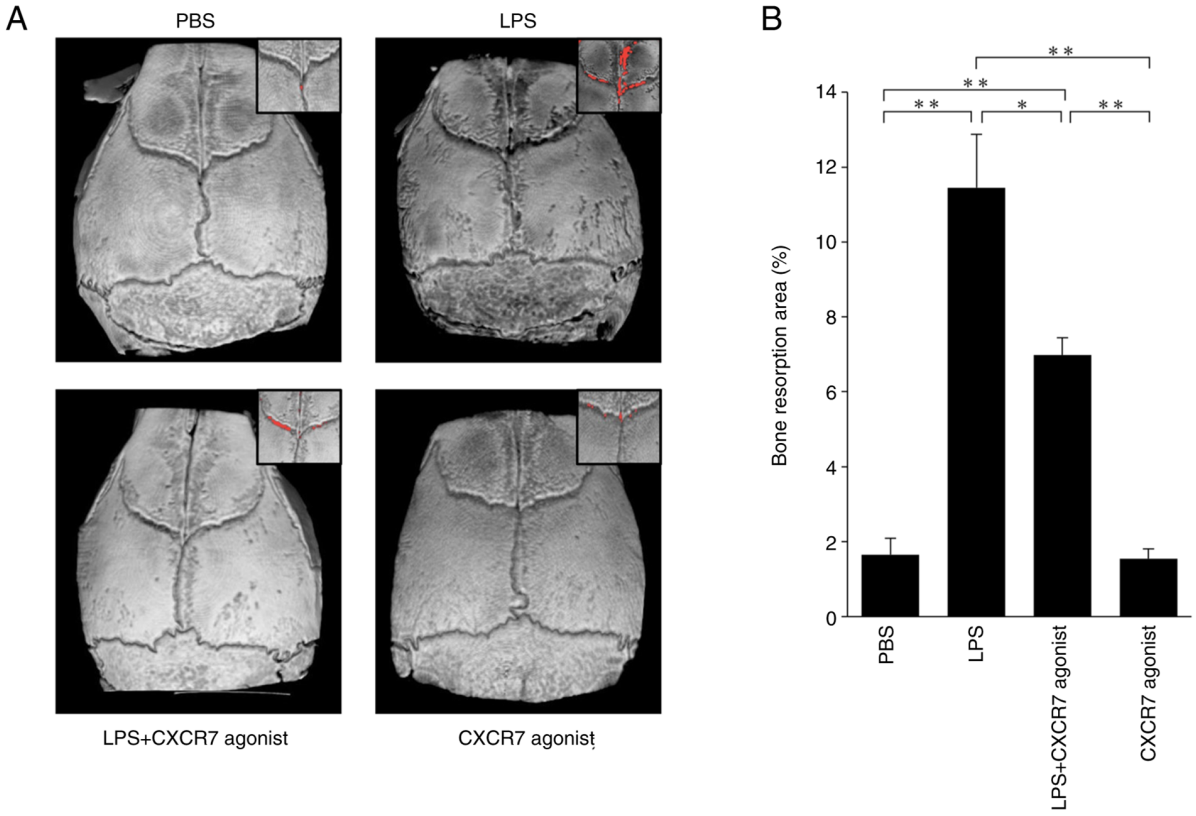

Figure 2. CXCR7 agonist as a C-X-C motif chemokine ligand 12 inhibitor ameliorates bone resorption induced by LPS injection *in vivo*. (A) Three-dimensional reconstructed image of mouse calvariae by micro-computed tomography. Red dots show the bone resorption area. (B) Ratio of bone resorption area to total bone area. The statistical significance of differences was determined by one-way ANOVA followed by Bonferroni/Dunn's test (n=4; *P<0.05, **P<0.01). Results are expressed as the mean ± SEM. CXCR7, C-X-C receptor 7; LPS, lipopolysaccharide; PBS, phosphate-buffered saline.

with the PBS-injected mice. The number of osteoclasts was significantly lower in mice treated with LPS+CXCR7 agonist than in mice treated with LPS alone (Fig. 1B). Both TRAP and Cathepsin K mRNA expression levels were significantly lower in mice injected with LPS+CXCR7 agonist than in mice injected with LPS alone (Fig. 1C and D).

CXCR7 agonist inhibits LPS-induced bone resorption in vivo. The bone resorption areas on mouse calvariae in each treated mouse were evaluated by micro-CT (Fig. 2A). LPS-treated mice showed a large area bone of resorption compared with the PBS-injected mice. The area of bone resorption was significantly smaller in mice treated with LPS+CXCR7 agonist than in mice injected with LPS alone (Fig. 2B).

CXCR7 agonist inhibits LPS-induced production of RANKL and TNF-α in vivo. The expression levels of RANKL and TNF-α mRNAs were significantly increased in LPS-treated mice compared with the PBS-injected mice. Furthermore, RANKL and TNF-α mRNA levels were significantly lower in mice treated with LPS+CXCR7 agonist compared with those administered with LPS alone (Fig. 3A and B).

CXCR7 agonist inhibits RANKL- and TNF-α-induced osteoclastogenesis through CXCL12 inhibition in vitro. The effects of CXCR7 agonist on RANKL- and TNF-α-induced osteoclastogenesis were assessed to investigate whether CXCR7 agonist affects osteoclast precursor cells via CXCL12. CXCL12 enhanced RANKL- and TNF-α-induced osteoclastogenesis. The number of osteoclasts was decreased in osteoclast precursor cells cultured with M-CSF+RANKL+CXCL12+CXCR7 agonist compared with M-CSF+RANKL+CXCL12 (Fig. 4A). The number of TRAP-positive osteoclasts was also decreased in cultures with M-CSF+TNF-α+CXCL12+CXCR7 agonist compared with M-CSF+TNF-α+CXCL12 (Fig. 4B).

Inhibitory effect of CXCR7 agonist on osteoclastogenesis via phosphorylation of MAPKs. The signal transduction pathway by which CXCR7 agonist inhibits osteoclastogenesis was examined. When RANKL or TNF-α was added to osteoclast precursors, the phosphorylation of MAPKs increased at 15 min. CXCL12 enhanced the phosphorylation of Erk when cells were treated with RANKL, but p-Erk expression was only slightly enhanced when cells were treated with TNF-α (Fig. 5A). Moreover, CXCR7 agonist reduced phosphorylation of Erk when cells were treated with RANKL or TNF-α and CXCL12 (Fig. 5A). However, no effect was observed on the phosphorylation of p38 and JNK (Fig. 5B and C).

Discussion

In the present study, the effects of a CXCR7 agonist as a CXCL12 inhibitor on osteoclastogenesis and bone resorption induced by LPS was analyzed *in vivo*. The CXCR7 agonist ameliorated osteoclastogenesis and bone resorption induced

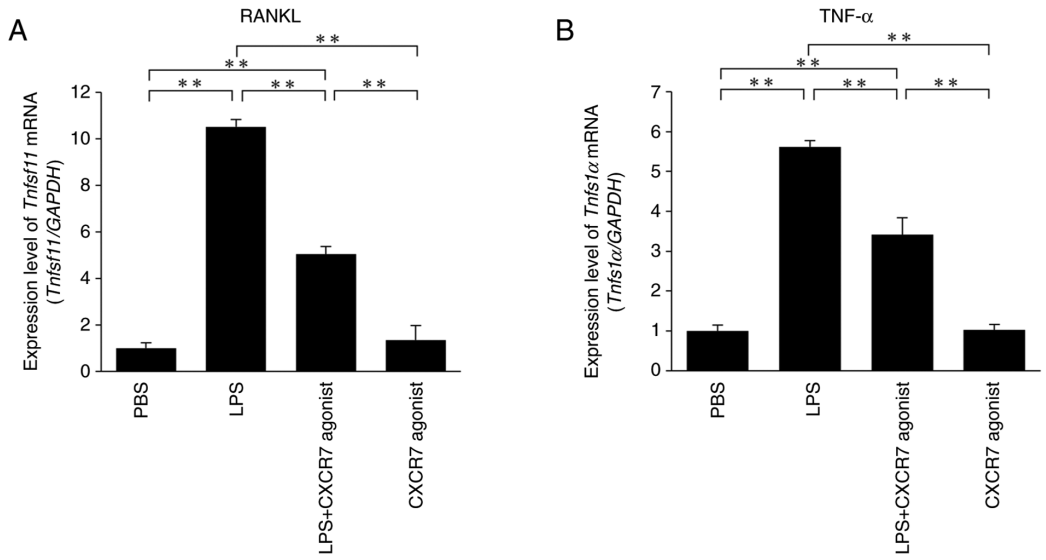

Figure 3. CXCR7 agonist inhibits the production of LPS-induced (A) RANKL and (B) TNF-α *in vivo*. The mRNA levels of RANKL and TNF-α in mouse calvariae were determined by reverse transcription-quantitative PCR. The statistical significance of differences was determined by one-way ANOVA followed by Bonferroni/Dunn's test (n=4; **P<0.01). Results are expressed as the mean ± SEM. CXCR7, C-X-C receptor 7; LPS, lipopolysaccharide; PBS, phosphate-buffered saline; RANKL, receptor activator of NF-κB ligand; TNF-α, tumor necrosis factor-α.

by LPS. Moreover, it was found that CXCR7 agonist inhibited the induction of RANKL and TNF-α expression by LPS *in vivo*. CXCR7 agonist inhibited RANKL-induced and TNF-α-induced osteoclastogenesis by inhibiting CXCL12 stimulation *in vitro*. CXCL12-mediated enhancement of osteoclastogenesis was inhibited by the CXCR7 agonist reducing the phosphorylation of Erk.

It has been reported that CXCL12-CXCR4-induced cellular events, such as angiogenesis, are negatively regulated by CXCR7 agonist (25). There have been no studies of the effects of CXCR7 agonists on osteoclastogenesis and bone resorption. To the best of our knowledge, the present study was the first to elucidate the effects of a CXCR7 agonist on LPS-induced osteoclastogenesis and bone resorption. A previous study showed that VUF11207 was a high affinity and potent ligand of CXCR7 (33), and this compound was used as a CXCR7 agonist in the present study.

CXCL12 plays important roles in patients with periodontitis and rheumatoid arthritis. CXCL12-CXCR4 signaling accelerates alveolar bone resorption (34). The interaction of CXCL12 and CXCR4 in patients with rheumatoid arthritis is important for cytokine production, angiogenesis and local inflammatory cell recruitment (35). Thus, CXCR4 signaling via CXCL12 enhances the differentiation and function of osteoclasts. However, whether CXCR7 agonists can inhibit the effects of CXCL12 is still unknown. VUF11207 is highly selective for CXCR7, suggesting that CXCR7 agonists may inhibit CXCL12-CXCR4 signaling (25).

LPS can induce systemic inflammation through interaction with CXCR4, activating the CXCL12/CXCR4 pathway (36). LPS can also modulate production of endogenous CXCL12 and CXCR4 (7). Our previous study showed that both CXCL12 and CXCR4 mRNA levels were increased in LPS-injected mice (22). In the present study, 100 μg/day of CXCR7 agonist was administered subcutaneously over the calvariae for 5 days. CXCR7 agonist inhibited osteoclastogenesis in the suture of the calvariae induced by LPS injection *in vivo*. TRAP and Cathepsin K mRNA levels were also lower in mice co-administered LPS and CXCR7 agonist compared with mice administered with LPS alone. The current study further investigated the inhibitory effect of CXCR7 agonist on bone resorption induced by LPS. The severity of bone destruction was evaluated by micro-CT through calculation of the ratio of bone destruction area to total area. It was found that the area of bone resorption was significantly lower in LPS and CXCR7 agonist-treated mice. These results suggested that CXCR7 agonist could attenuate osteoclastogenesis and bone resorption induced by LPS *in vivo*. These results regarding the effects of a CXCR7 agonist on osteoclastogenesis were similar to those of a previous study indicating that a CXCR7 agonist inhibited CXCL12-induced angiogenesis (25).

LPS induces RANKL expression from osteoblasts and production of proinflammatory cytokines, such as TNF-α and IL-1, from macrophages and other cells (37). It has been reported that periodontal ligament cells also express numerous types of proinflammatory cytokines to regulate osteoclastogenesis by LPS (38). RANKL and TNF-α contribute to LPS-induced osteoclastogenesis and bone resorption (39). In the present study, RANKL and TNF-α mRNA levels were significantly lower in mice co-administered LPS and CXCR7 agonist compared with mice administered with LPS alone. Furthermore, our previous study showed that CXCL12 directly enhanced both RANKL- and TNF-α-induced osteoclast differentiation (22). In the present study, CXCR7 agonist was added to this culture system to investigate the effects of CXCR7 agonist on RANKL- and TNF-α-induced osteoclastogenesis. It was found that the CXCR7 agonist suppressed osteoclastogenesis enhanced by CXCL12. These results suggested that one of the mechanisms underlying the inhibitory effect of CXCR7 on osteoclastogenesis induced by LPS may be decreased levels of osteoclast-associated cytokines induced by LPS *in vivo*. Another mechanism may

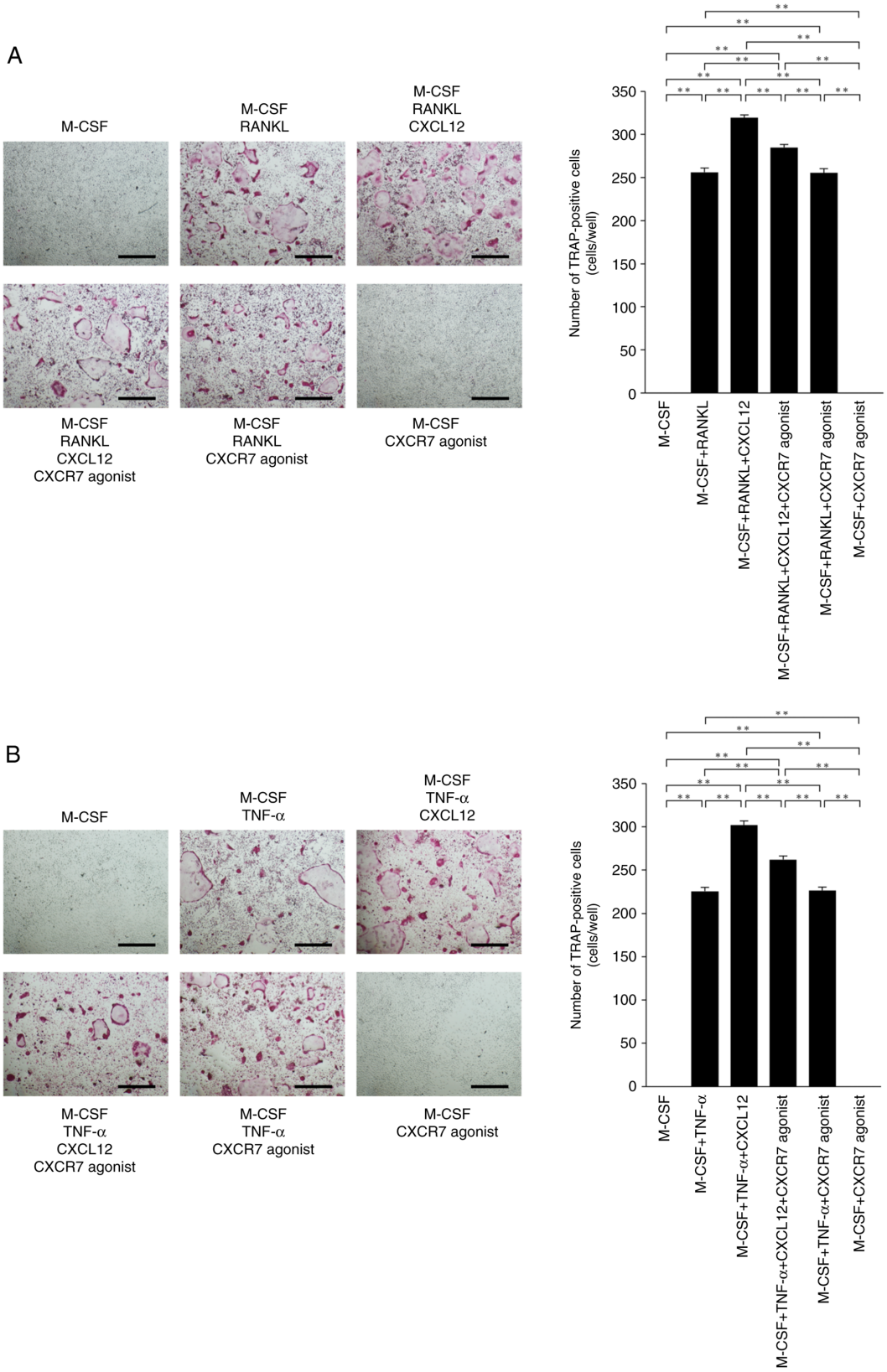

Figure 4. CXCR7 agonist inhibits RANKL-induced and TNF-α-induced osteoclastogenesis through CXCL12 inhibition. (A) Microscopic images and number of osteoclasts. Osteoclast precursors were treated for 5 days with one of the following and then stained for TRAP: i) M-CSF (100 ng/ml); ii) M-CSF (100 ng/ml) + RANKL (50 ng/ml); iii) M-CSF (100 ng/ml) + RANKL (50 ng/ml) + CXCL12 (100 ng/ml); iv) M-CSF (100 ng/ml) + RANKL (50 ng/ml) + CXCL12 (100 ng/ml) + CXCR7 agonist (100 ng/ml); v) M-CSF (100 ng/ml) + RANKL (50 ng/ml) + CXCR7 agonist (100 ng/ml); or vi) M-CSF (100 ng/ml) + CXCR7 agonist (100 ng/ml). (B) Microscopic images and number of osteoclasts. Osteoclast precursors were treated for 5 days with one of the following and then stained for TRAP: i) M-CSF (100 ng/ml); ii) M-CSF (100 ng/ml) + TNF-α (50 ng/ml); iii) M-CSF (100 ng/ml) + TNF-α (50 ng/ml) + CXCL12 (100 ng/ml); iv) M-CSF (100 ng/ml) + TNF-α (50 ng/ml) + CXCL12 (100 ng/ml) + CXCR7 agonist (100 ng/ml); v) M-CSF (100 ng/ml) + TNF-α (50 ng/ml) + CXCR7 agonist (100 ng/ml); or vi) M-CSF (100 ng/ml) + CXCR7 agonist (100 ng/ml). Scale bar, 500 μm. The statistical significance of differences was determined by one-way ANOVA followed by Bonferroni/Dunn's test (n=4; **P<0.01). Results are expressed as the mean ± SEM. CXCR7, C-X-C receptor 7; CXCL12, C-X-C motif chemokine ligand 12; TRAP, tartrate-resistant acid phosphatase; RANKL, receptor activator of NF-κB ligand; TNF-α, tumor necrosis factor-α; M-CSF, macrophage colony stimulating factor.

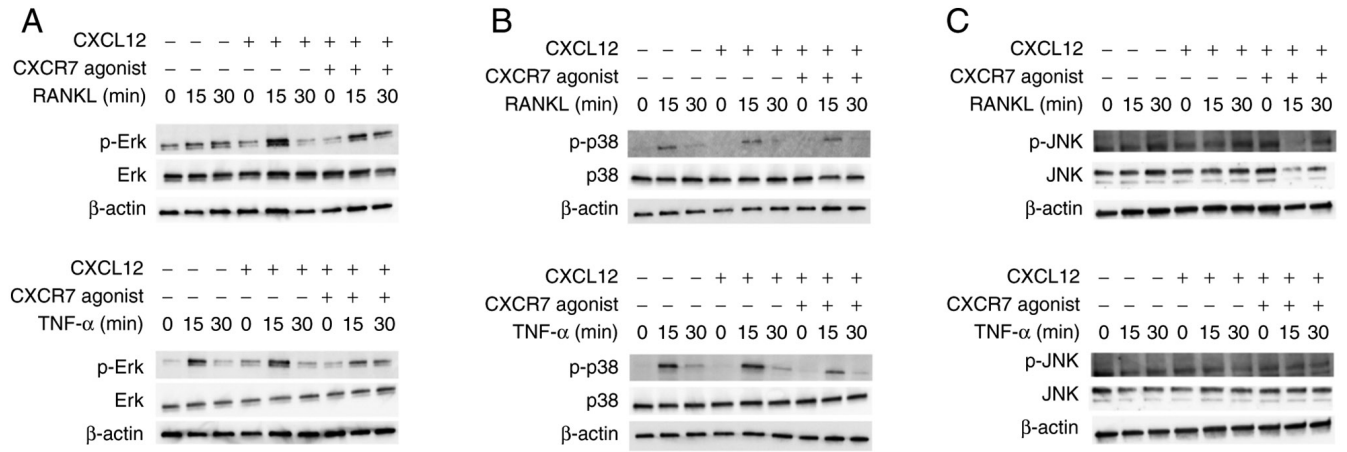

Figure 5. CXCR7 agonist inhibits phosphorylation of Erk. Osteoclast precursors were incubated with RANKL, TNF-α, CXCL12 and CXCR7 agonist. Cells were lysed and the contents were analyzed by immunoblotting using the following antibodies: (A) p-Erk and Erk, (B) p-p38 and p38, and (C) p-JNK and JNK. CXCR7, C-X-C receptor 7; CXCL12, C-X-C motif chemokine ligand 12; RANKL, receptor activator of NF-κB ligand; TNF-α, tumor necrosis factor-α; p-, phosphorylated.

involve CXCR7 agonist-mediated inhibition of RANKL- and TNF-α-induced osteoclastogenesis via inhibition of CXCL12. Furthermore, CXCR7 agonists may indirectly inhibit osteoclastogenesis *in vivo*.

CXCR7 transduces signals via the β-arrestin pathway rather than the G protein-mediated pathway (40). It has been reported that CXCL12 leads to the phosphorylation of Erk in CXCR7-positive glioma cells (41). We hypothesized that CXCL12 and CXCR7 agonist may regulate the phosphorylation of MAPKs in osteoclast precursors. In the present study, immunoblotting was performed to investigate signal transduction. CXCL12 enhanced phosphorylation of Erk when osteoclast precursors were treated with RANKL or TNF-α. This result suggested that CXCL12 enhanced phosphorylation in osteoclast precursors as well as in glioma cells. Moreover, CXCR7 agonist reduced phosphorylation of Erk. These results were consistent with the inhibitory effect of CXCR7 agonist on osteoclastogenesis *in vitro*. Therefore, suppression of CXCL12-enhanced phosphorylation of Erk was considered to play a major role in the inhibitory effect of CXCR7 agonist on osteoclastogenesis.

CXCL12 is associated with various diseases, and CXCR7 agonists have been shown to be useful in these diseases (42). The findings of the present study suggested that CXCR7 agonists have the potential to suppress inflammation by CXCL12-enhanced osteoclastogenesis. To confirm the role of CXCR7 agonists in more detail, further analysis including knockout mice should be performed in the future. It was concluded that CXCR7 agonists inhibited osteoclastogenesis and bone resorption induced by LPS *in vivo*. Furthermore, CXCR7 agonists also inhibited RANKL- and TNF-α-induced osteoclastogenesis by inhibiting CXCL12-mediated enhancement of osteoclastogenesis *in vitro*. The underlying mechanisms through which CXCR7 agonists attenuated osteoclastogenesis and bone destruction induced by LPS *in vivo* appeared to be related to inhibitory effects on LPS-induced TNF-α and RANKL expression *in vivo*, as well as on RANKL- and TNF-α-induced osteoclastogenesis *in vitro* via inhibition of CXCL12-mediated upregulation of osteoclastogenesis.

Acknowledgements

Not applicable.

Funding

This research was funded by the Japan Society for the Promotion of Science Grants-in-Aid for Scientific Research (JSPS KAKENHI; grant nos. 16K11776, 19K10397 and 18K09862).

Availability of data and materials

The datasets used and/or analyzed during the current study are available from the corresponding author on reasonable request.

Authors' contributions

APN, HK, FO and IM contributed to the conception and design of this study, data acquisition, analysis and interpretation, and drafting of the manuscript. HK, APN and FO contributed to critical revision of the manuscript. APN, HK and FO confirm the authenticity of all the raw data. AP, SO, TN, AM, YN and RK collected the samples and performed data analysis. HK and IM supervised the project. All authors read and approved the final manuscript.

Ethics approval and consent to participate

All experimental procedures conformed to 'Regulations for Animal Experiments and Related Activities at Tohoku University', and were reviewed by the Institutional Laboratory Animal Care and Use Committee of Tohoku University, and finally approved by the President of University (approval no. 2019DnA-047-05; Miyagi, Japan).

Patient consent for publication

Not applicable.

Competing interests

The authors declare that they have no competing interests.

References

1. Boyce BF, Li J, Xing L and Yao Z: Bone remodeling and the role of TRAF3 in osteoclastic bone resorption. Front Immunol 9: 2263, 2018.
2. Crotti TN, Dharmapatni AA, Alias E and Haynes DR: Osteoimmunology: Major and costimulatory pathway expression associated with chronic inflammatory induced bone loss. J Immunol Res 2015: 281287, 2015.
3. Teitelbaum SL: Bone resorption by osteoclasts. Science 289: 1504-1508, 2000.
4. Azuma Y, Kaji K, Katogi R, Takeshita S and Kudo A: Tumor necrosis factor-alpha induces differentiation of and bone resorption by osteoclasts. J Biol Chem 275: 4858-4864, 2000.
5. Kobayashi K, Takahashi N, Jimi E, Udagawa N, Takami M, Kotake S, Nakagawa N, Kinosaki M, Yamaguchi K, Shima N, *et al*: Tumor necrosis factor alpha stimulates osteoclast differentiation by a mechanism independent of the ODF/RANKL-RANK interaction. J Exp Med 191: 275-286, 2000.
6. Kitaura H, Zhou P, Kim HJ, Novack DV, Ross FP and Teitelbaum SL: M-CSF mediates TNF-induced inflammatory osteolysis. J Clin Invest 115: 3418-3427, 2005.
7. Xing Q, de Vos P, Faas MM, Ye Q and Ren Y: LPS promotes pre-osteoclast activity by up-regulating CXCR4 via TLR-4. J Dent Res 90: 157-162, 2011.
8. Islam S, Hassan F, Tumurkhuu G, Dagvadorj J, Koide N, Naiki Y, Mori I, Yoshida T and Yokochi T: Bacterial lipopolysaccharide induces osteoclast formation in RAW 264.7 macrophage cells. Biochem Biophys Res Commun 360: 346-351, 2007.
9. Mörmann M, Thederan M, Nackchbandi I, Giese T, Wagner C and Hänsch GM: Lipopolysaccharides (LPS) induce the differentiation of human monocytes to osteoclasts in a tumour necrosis factor (TNF) alpha-dependent manner: A link between infection and pathological bone resorption. Mol Immunol 45: 3330-3337, 2008.
10. Zou W and Bar-Shavit Z: Dual modulation of osteoclast differentiation by lipopolysaccharide. J Bone Miner Res 17: 1211-1218, 2002.
11. Kimura K, Kitaura H, Fujii T, Hakami ZW and Takano-Yamamoto T: Anti-c-Fms antibody inhibits lipopolysaccharide-induced osteoclastogenesis in vivo. FEMS Immunol Med Microbiol 64: 219-227, 2012.
12. Kikuchi T, Matsuguchi T, Tsuboi N, Mitani A, Tanaka S, Matsuoka M, Yamamoto G, Hishikawa T, Noguchi T and Yoshikai Y: Gene expression of osteoclast differentiation factor is induced by lipopolysaccharide in mouse osteoblasts via Toll-like receptors. J Immunol 166: 3574-3579, 2001.
13. Lee J, Park C, Kim HJ, Lee YD, Lee ZH, Song YW and Kim HH: Stimulation of osteoclast migration and bone resorption by C-C chemokine ligands 19 and 21. Exp Mol Med 49: e358, 2017.
14. Votta BJ, White JR, Dodds RA, James IE, Connor JR, Lee-Rykaczewski E, Eichman CF, Kumar S, Lark MW and Gowen M: CKbeta-8 [CCL23], a novel CC chemokine, is chemotactic for human osteoclast precursors and is expressed in bone tissues. J Cell Physiol 183: 196-207, 2000.
15. Watanabe K, Penfold ME, Matsuda A, Ohyanagi N, Kaneko K, Miyabe Y, Matsumoto K, Schall TJ, Miyasaka N and Nanki T: Pathogenic role of CXCR7 in rheumatoid arthritis. Arthritis Rheum 62: 3211-3220, 2010.
16. Puchert M and Engele J: The peculiarities of the SDF-1/CXCL12 system: In some cells, CXCR4 and CXCR7 sing solos, in others, they sing duets. Cell Tissue Res 355: 239-253, 2014.
17. Chen D, Xia Y, Zuo K, Wang Y, Zhang S, Kuang D, Duan Y, Zhao X and Wang G: Crosstalk between SDF-1/CXCR4 and SDF-1/CXCR7 in cardiac stem cell migration. Sci Rep 5: 16813, 2015.
18. Okada K, Kawao N, Yano M, Tamura Y, Kurashimo S, Okumoto K, Kojima K and Kaji H: Stromal cell-derived factor-1 mediates changes of bone marrow stem cells during the bone repair process. Am J Physiol Endocrinol Metab 310: E15-E23, 2016.
19. Teixido J, Martinez-Moreno M, Diaz-Martinez M and Sevilla-Movilla S: The good and bad faces of the CXCR4 chemokine receptor. Int J Biochem Cell Biol 95: 121-131, 2018.
20. Dong Y, Liu H, Zhang X, Xu F, Qin L, Cheng P, Huang H, Guo F, Yang Q and Chen A: Inhibition of SDF-1α/CXCR4 signalling in subchondral bone attenuates post-traumatic osteoarthritis. Int J Mol Sci 17: 943, 2016.
21. Pawig L, Klasen C, Weber C, Bernhagen J and Noels H: Diversity and inter-connections in the CXCR4 chemokine receptor/ligand family: Molecular perspectives. Front Immunol 6: 429, 2015.
22. Shima K, Kimura K, Ishida M, Kishikawa A, Ogawa S, Qi J, Shen WR, Ohori F, Noguchi T, Marahleh A and Kitaura H: C-X-C Motif Chemokine 12 enhances lipopolysaccharide-induced osteoclastogenesis and bone resorption in vivo. Calcif Tissue Int 103: 431-442, 2018.
23. Luo T, Liu H, Feng W, Liu D, Du J, Sun J, Wang W, Han X, Guo J, Amizuka N, *et al*: Adipocytes enhance expression of osteoclast adhesion-related molecules through the CXCL12/CXCR4 signalling pathway. Cell Prolif 50: e12317, 2017.
24. Hatano K, Ishida Y, Yamaguchi H, Hosomichi J, Suzuki JI, Usumi-Fujita R, Shimizu Y, Shibutani N, Kaneko S and Ono T: The chemokine receptor type 4 antagonist, AMD3100, interrupts experimental tooth movement in rats. Arch Oral Biol 86: 35-39, 2018.
25. Uto-Konomi A, McKibben B, Wirtz J, Sato Y, Takano A, Nanki T and Suzuki S: CXCR7 agonists inhibit the function of CXCL12 by down-regulation of CXCR4. Biochem Biophys Res Commun 431: 772-776, 2013.
26. McHugh KP, Hodivala-Dilke K, Zheng MH, Namba N, Lam J, Novack D, Feng X, Ross FP, Hynes RO and Teitelbaum SL: Mice lacking beta3 integrins are osteosclerotic because of dysfunctional osteoclasts. J Clin Invest 105: 433-440, 2000.
27. Kitaura H, Sands MS, Aya K, Zhou P, Hirayama T, Uthgenannt B, Wei S, Takeshita S, Novack DV, Silva MJ, *et al*: Marrow stromal cells and osteoclast precursors differentially contribute to TNF-alpha-induced osteoclastogenesis in vivo. J Immunol 173: 4838-4846, 2004.
28. Takeshita S, Kaji K and Kudo A: Identification and characterization of the new osteoclast progenitor with macrophage phenotypes being able to differentiate into mature osteoclasts. J Bone Miner Res 15: 1477-1488, 2000.
29. Saeed J, Kitaura H, Kimura K, Ishida M, Sugisawa H, Ochi Y, Kishikawa A and Takano-Yamamoto T: IL-37 inhibits lipopolysaccharide-induced osteoclast formation and bone resorption in vivo. Immunol Lett 175: 8-15, 2016.
30. Ishida M, Kitaura H, Kimura K, Sugisawa H, Aonuma T, Takada H and Takano-Yamamoto T: Muramyl dipeptide enhances lipopolysaccharide-induced osteoclast formation and bone resorption through increased RANKL expression in stromal cells. J Immunol Res 2015: 132765, 2015.
31. Livak KJ and Schmittgen TD: Analysis of relative gene expression data using real-time quantitative PCR and the 2(-Delta Delta C(T)) method. Methods 25: 402-408, 2001.
32. Ohori F, Kitaura H, Ogawa S, Shen WR, Qi J, Noguchi T, Marahleh A, Nara Y, Pramusita A and Mizoguchi I: IL-33 inhibits TNF-α-induced osteoclastogenesis and bone resorption. Int J Mol Sci 21: 1130, 2020.
33. Wijtmans M, Maussang D, Sirci F, Scholten DJ, Canals M, Mujić-Delić A, Chong M, Chatalic KL, Custers H, Janssen E, *et al*: Synthesis, modeling and functional activity of substituted styrene-amides as small-molecule CXCR7 agonists. Eur J Med Chem 51: 184-192, 2012.
34. Nagashima H, Shinoda M, Honda K, Kamio N, Hasuike A, Sugano N, Arai Y, Sato S and Iwata K: CXCR4 signaling contributes to alveolar bone resorption in *Porphyromonas gingivalis*-induced periodontitis in mice. J Oral Sci 59: 571-577, 2017.
35. Pablos JL, Santiago B, Galindo M, Torres C, Brehmer MT, Blanco FJ and García-Lázaro FJ: Synoviocyte-derived CXCL12 is displayed on endothelium and induces angiogenesis in rheumatoid arthritis. J Immunol 170: 2147-2152, 2003.
36. Yang L, Wang M, Guo YY, Sun T, Li YJ, Yang Q, Zhang K, Liu SB, Zhao MG and Wu YM: Systemic inflammation induces anxiety disorder through CXCL12/CXCR4 pathway. Brain Behav Immun 56: 352-362, 2016.

37. Kitaura H, Ishida M, Kimura K, Sugisawa H, Kishikawa A, Shima K, Ogawa S, Qi J and Shen WR: Role of muramyl dipeptide in lipopolysaccharide-mediated biological activity and osteoclast activity. Anal Cell Pathol (Amst) 2018: 8047610, 2018.
38. Lee SY, Moon JS, Yang DW, Yoo HI, Jung JY, Kim OS, Kim MS, Koh JT, Chung HJ and Kim SH: SLPI in periodontal Ligament is not sleepy during biophysical force-induced tooth movement. J Clin Periodontol 48: 528-540, 2021.
39. Ishida M, Shen WR, Kimura K, Shima K, Ogawa S, Qi J, Ohori F, Noguchi T, Marahleh A and Kitaura H: DPP-4 inhibitor impedes lipopolysaccharide-induced osteoclast formation and bone resorption in vivo. Biomed Pharmacother 109: 242-253, 2019.
40. Rajagopal S, Kim J, Ahn S, Craig S, Lam CM, Gerard NP, Gerard C and Lefkowitz RJ: Beta-arrestin-but not G protein-mediated signaling by the 'decoy' receptor CXCR7. Proc Natl Acad Sci USA 107: 628-632, 2010.
41. Hattermann K, Held-Feindt J, Lucius R, Müerköster SS, Penfold ME, Schall TJ and Mentlein R: The chemokine receptor CXCR7 is highly expressed in human glioma cells and mediates antiapoptotic effects. Cancer Res 70: 3299-3308, 2010.
42. Lounsbury N: Advances in CXCR7 modulators. Pharmaceuticals (Basel) 13: 33, 2020.